Article

The Bmp Gradient of the Zebrafish Gastrula Guides Migrating Lateral Cells by Regulating Cell-Cell Adhesion

Sophia von der Hardt,[1] Jeroen Bakkers,[1,5] Adi Inbal,[2]
Lara Carvalho,[3] Lilianna Solnica-Krezel,[2]
Carl-Philipp Heisenberg,[3]
and Matthias Hammerschmidt[1,4,*]
[1] Max-Planck Institute of Immunobiology
D-79108 Freiburg
Germany
[2] Vanderbilt University
Nashville, Tennessee 37235
[3] Max-Planck Institute of Molecular Cell Biology
 and Genetics
D-01307 Dresden
Germany
[4] Institute for Developmental Biology
Cologne University
D-50923 Cologne
Germany

Summary

Background: Bone morphogenetic proteins (Bmps) are required for the specification of ventrolateral cell fates during embryonic dorsoventral patterning and for proper convergence and extension gastrulation movements, but the mechanisms underlying the latter role remained elusive.

Results: Via bead implantations, we show that the Bmp gradient determines the direction of lateral mesodermal cell migration during dorsal convergence in the zebrafish gastrula. This effect is independent of its role during dorsoventral patterning and of noncanonical Wnt signaling. However, it requires Bmp signal transduction through Alk8 and Smad5 to negatively regulate Ca^{2+}/Cadherin-dependent cell-cell adhesiveness. In vivo, converging mesodermal cells form lamellipodia that attach to adjacent cells. Bmp signaling diminishes the Cadherin-dependent stability of such contact points, thereby abrogating subsequent cell displacement during lamellipodial retraction.

Conclusions: We propose that the ventral-to-dorsal Bmp gradient has an instructive role to establish a reverse gradient of cell-cell adhesiveness, thereby defining different migratory zones and directing lamellipodia-driven cell migrations during dorsal convergence in lateral regions of the zebrafish gastrula.

Introduction

During fish and amphibian gastrulation, different morphogenetic movements take place that modify the overall shape and architecture of the embryo: epiboly, involution, convergence, and extension [1]. Convergence and extension movements result in mediolateral narrowing and anteroposterior elongation of the nascent embryonic axis, driven by a combination of cell behaviors that vary according to position in the gastrula and stage of development (see [2] for review).

Convergence and extension movements of the lateral mesoderm of zebrafish embryos are largely based on lamellipodia-driven cell migrations, which depend on Rac1-mediated Hyaluronan signaling [3]. At midgastrula stages, when cells are in ventrolateral positions, they move more slowly and less directed than later, when they have reached more dorsolateral regions and have become mediolaterally elongated [2, 4–6]. As mediolateral intercalation of the mesoderm within the dorsal axis, the late and fast migration of lateral mesodermal cells in dorsolateral regions requires noncanonical Wnt signaling [6], Stat3 [7, 8], and the G proteins $G\alpha12/13$ [9]. Interestingly, $G\alpha12/13$ predominantly regulate migration directionality. This has led to the suggestion that they might mediate signaling by a chemo-attractant from the dorsal midline, which had also been proposed from mathematical modeling [6]. Stat3 and $G\alpha12/13$ are also required for the earlier and slower migration of mesodermal cells in ventrolateral positions, whereas noncanonical Wnt signaling is not [6], suggesting that here other or additional regulatory systems are at play. Finally, cells in ventral-most positions do not move dorsally at all, defining the so-called no-convergence-no-extension zone [4].

The ventral no-convergence-no-extension zone as well as the ventrolateral migratory domain are altered in size in *chordin* and *smad5* mutants [5], pointing to a regulation by Bone morphogenetic protein (Bmp) signaling. Bmps are members of the Tgfβ superfamily. During zebrafish gastrulation, three different *bmp* genes are expressed, *bmp2b*, *bmp4*, and *bmp7*, all of which show highest expression levels on the ventral side and progressively decreasing levels toward the dorsal axis. Analyses of mutants in Bmp2b, Bmp7, their type I receptor Alk8, their downstream transcription factor Smad5, and their dorsal inhibitor Chordin have shown that Bmp signaling is required for the specification of ventrolateral cell fates. Loss of Bmp signaling leads to a loss or reduction of derivatives of the ventral mesoderm such as blood and pronephric precursor cells, while the domain of muscle precursor cells, derivatives of the paraxial mesoderm, is expanded ventrally (see [10] for review). This is in contrast to the aforementioned convergence and extension regulators, which do not affect dorsoventral patterning. Hence, it remained largely unclear whether the convergence defects upon gain or loss of Bmp signaling are secondary consequences of the shifts in dorsoventral patterning or whether they reflect an independent, parallel role of Bmp signaling.

Here, we show that Bmp signaling has a repulsive effect on migrating lateral mesodermal cells, which is independent of its role on dorsoventral patterning and of noncanonical Wnt signaling. Unlike other chemotactic agents, Bmp signaling does not regulate the protrusive

*Correspondence: hammerschmid@immunbio.mpg.de
[5] Present address: Hubrecht Institute, 3584 CT Utrecht, The Netherlands.

activity of migrating cells. Rather, it diminishes calcium-dependent cell-cell adhesion in a Smad5-dependent manner, most likely via transcriptional control of a thus far unidentified target gene. Such cell adhesion is important for lamellipodia-driven migration of lateral mesodermal cells, as shown by the fact that the protrusions attach to adjacent cells, followed by a cell displacement into this direction, if the cell-cell contact is strong enough. We propose a model according to which the Bmp gradient, by regulating cell-cell adhesiveness, subdivides the gastrula in different migratory zones. In ventral-most regions, where Bmp signaling is highest, low adhesiveness results in no convergence and no extension. In ventrolateral regions, however, decreasing Bmp concentrations set up a reverse gradient of cell-cell adhesiveness, making cells move into dorsal regions, where adhesiveness is highest.

Results

The Bmp Gradient Determines the Direction of Convergence Movements

Recordings of groups of fluorescently labeled lateral mesodermal cells throughout gastrulation revealed that both early and late convergence movements (Figure 1B) were abolished when the dorsoventral Bmp gradient (Figure 1A) was disrupted, either by Bmp overexpression (injection of *bmp2b* mRNA and *chordin* antisense morpholino oligonucleotide [MO]), generating embryos with homogeneously high Bmp signaling (Figures 1C and 1D; n = 12/12), or by knocking down Bmp signaling (injection of *bmp2b*-MO), generating embryos that lack Bmp signaling along the entire dorsoventral axis (Figures 1E and 1F; n = 15/15).

To generate artificial Bmp activity gradients, beads loaded with Bmp proteins were implanted into *bmp2b* morphants at early gastrula (shield) stages. Whereas implantation into ventrolateral positions restored normal dorsal convergence (Figures 1G and 1H; n = 8/8), beads implanted into dorsolateral positions generated a reverse Bmp gradient and made cells move into the opposite, ventral direction (Figures 1I and 1J; n = 12/12). In contrast, cells did not respond to implanted control beads loaded with BSA (n = 7/7; see Figures S1A and S1B in the Supplemental Data available online). Together, these results suggest that converging lateral cells are guided by and move down the Bmp gradient.

Slow Convergence Requires Bmp Signaling in the Environment and Is Independent of Noncanonical Wnt and Fgf Signaling

To study whether the cell-guiding effect of Bmps requires their type I receptor Alk8 [11, 12] and downstream transcription factor Smad5 [13], we implanted Bmp beads into *alk8* or *smad5* morphant embryos. In striking contrast to *bmp2* morphants (Figure 1J) or even *bmp2b/4/7* triple morphant embryos (Figures S1E and S1F; n = 4/4), cells in *alk8* or *smad5* morphants failed to move away from the bead (Figure 1L; Figures S1C and S1D; n = 10/10), suggesting that transcriptional activation is needed for Bmp-mediated cell migration. However, *alk8* morphant cells did move away from the bead when transplanted into *bmp2b* morphant hosts (Figure 1K; n = 5/5), whereas *bmp2b* morphant cells transplanted into *alk8* morphant hosts did not (Figure 1L; n = 6/6). This suggests that cells do not necessarily have to receive the Bmp signal themselves to be able to move away from the Bmp source. Rather, it seems to be the establishment of a Bmp gradient in the environment that is required to determine the direction of cell movements.

To exclude the possibility that the effects are caused by transcriptional regulation of downstream signaling factors previously described to be involved in convergence and extension movements, we tested Bmp beads in combination with various MOs or inhibitory drugs. Thus, Bmp beads were implanted into *bmp2b* morphants that had either been coinjected with *wnt5a* MO and *wnt11* MO (Figure S1G; n = 7/7) or been treated with the Fgf receptor-blocking agent SU5402 [14] (Figure S1J; n = 6/6). In both cases, lateral cells moved away from the bead, although in situ hybridizations of sibling embryos revealed defects characteristic for loss of noncanonical Wnt or Fgf signaling (Figures S1H, S1I, S1K, and S1L). This indicates that Bmp-mediated cell guidance is independent of noncanonical Wnt and Fgf signaling. In the same manner, we ruled out an involvement of PI3K or PDGF signaling by applying 20 μM SU4984 [15] or 30 μM LY294002 [16], respectively (data not shown).

Bmp Signaling Can Affect Dorsal Convergence Independently of Dorsoventral Cell-Fate Specification

Bmp signaling is required for the establishment of ventrolateral and the suppression of dorsal cell fates. Thus, *bmp2b* morphants lack expression of the ventral marker gene *eve1* [17], while expression of *tbx24* [18], a marker for dorsolateral, presumptive paraxial mesoderm, is expanded into ventral-most regions (compare Figures 2B and 2H with Figures 2A and 2G). Implantation of a Bmp bead into dorsolateral regions of a *bmp2b* morphant led to long-range clearance of *tbx24* expression (Figure 2C). However, the bead failed to induce *eve1* expression (Figure 2C), indicating that it does not recapitulate the whole spectrum of dorsoventral fates, but creates a large field of laterally specified mesodermal cells, as normally only found at 90° from the dorsal side (Figures 2A, 2D, and 2G). This indicates that the Bmp bead can induce convergence movements without inducing ventral-most cell fates.

Support for a role of Bmp signaling during dorsal convergence generally independent of dorsoventral patterning came from genetic interaction assays between *bmp2b* and *has2,* encoding Hyaluronan synthase 2. *has2* is required for lamellipodia formation and cell migration during dorsal convergence movements, but is, in contrast to *bmp2b*, dispensable for dorsoventral cell-fate specification [3]. When injecting low amounts of *has2* MO into *bmp2b* heterozygotes, we obtained strong defects in dorsal convergence of lateral mesodermal cells (Figure 3C; n = 7/8), comparable to those of *bmp2b* morphants (Figure 1F), although both uninjected *bmp2b* heterozygotes (Figure 3A; n = 7/7) and wild-type embryos injected with the same low amounts of *has2* MO (Figure 3B; n = 15/15) showed normal convergence behavior. In contrast, shifts in dorsoventral cell-fate specification of *bmp2b* heterozygotes injected
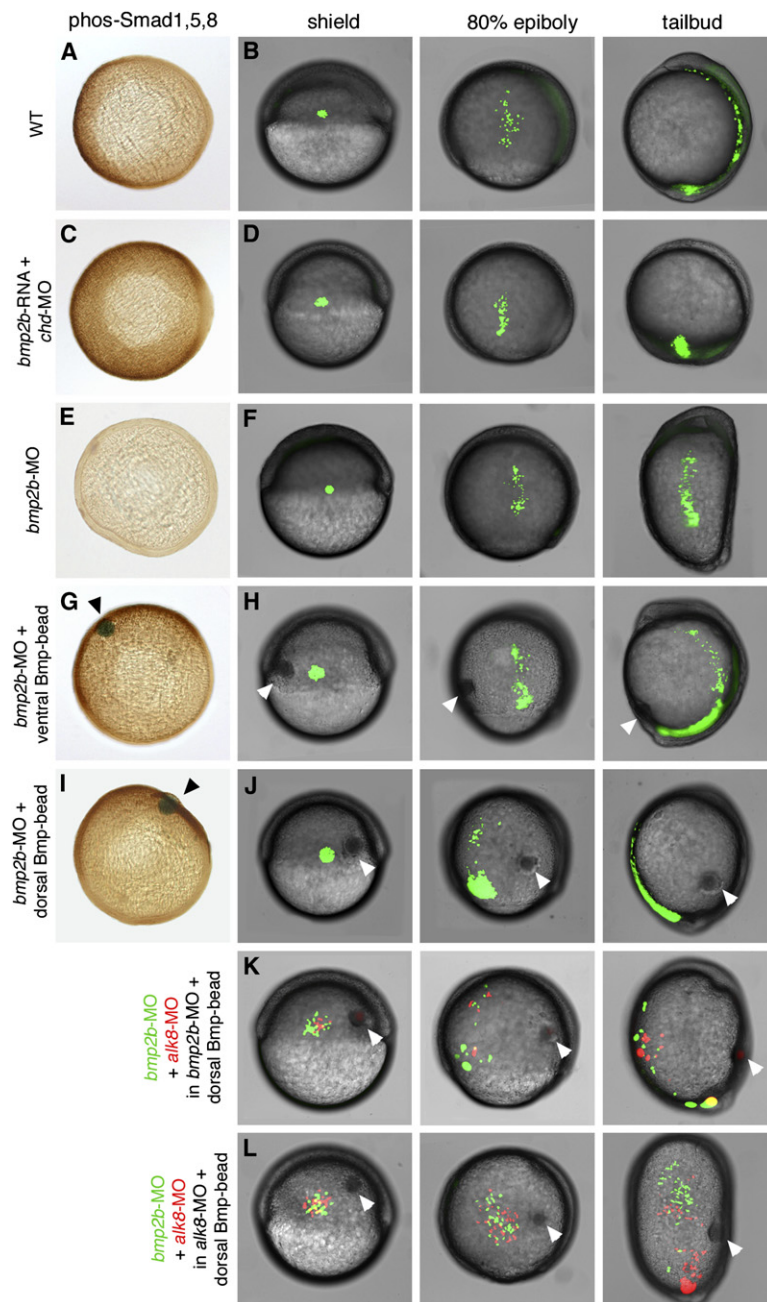
Figure 1. The Bmp Gradient Determines the Direction of Cell Movements during Dorsal Convergence of the Lateral Mesoderm in a Non-Cell-Autonomous Fashion

(A, C, E, G, and I) Vegetal views of embryos at 85% epiboly after anti-phospho Smad1/5 immunostainings, dorsal to the right.

(B, D, F, H, J–L) All other panels show live embryos after photoactivation of caged fluorescent dextran in a group of cells in the lateral mesoderm (B, D, F, H, and J) or after transplantation of a mixture of lateral mesodermal cells containing fluorescein or rhodamin dextran (K and L).

Each embryo is shown at shield stage (early gastrula, 6 hpf), at 80% epiboly stage (midgastrula, 8 hpf), and at tailbud stage (end of gastrulation, 10 hpf). Dorsal is to the right, anterior/animal pole at the top. Embryos were injected either with *bmp2b* mRNA and *chordin* MO (C and D), with *bmp2b* MO (E–K), or with *alk8* MO (L). To restore or generate a reverse Bmp gradient, Bmp beads (marked with arrowheads) were implanted into ventrolateral (G and H) or dorsolateral (I–L) positions of *bmp2b* or *alk8* morphants at shield stage.

with low amounts of *has2* MO were not more severe than in uninjected heterozygous embryos, as revealed by unaltered transcript levels of the ventral marker genes *sizzled* and *gata1* at late gastrula and midsegmentation stages (determined via quantitative RT-PCR; Figures S2A and S2C) and by unaltered numbers of *pax2.1*- and *gata1*-positive pronephric duct and blood precursor cells (determined via in situ hybridization; Figure 3G; n = 11/11; and data not shown, n = 9/9).

High Bmp Signaling Leads to an Uncoupling of Lamellipodial Retraction and Cell Body Displacement

In order to understand why loss and gain of *bmp2b* impair convergence movements, we performed time-lapse studies, tracking individual mesodermal cells during

gastrulation. At 80%–85% epiboly, movements of wild-type lateral mesodermal cells were already reasonably directed toward the axis (Figures 4A and 4D). In contrast, upon both gain and loss of Bmp signaling, cells displayed a strong reduction in net dorsal movement (Figure 4D). However, the cell behavior defects leading to this same net result were different. Whereas *bmp2b* morphant cells moved in random directions with unaltered speed, cells overexpressing *bmp2b* displayed a strong reduction in velocity (Figures 4B–4D).

Migration of lateral mesodermal cells depends on lamellipodia [3]. However, we found that *bmp2b* morphant as well as *bmp2b*-overexpressing cells form lamellipodia in shapes and numbers similar to wild-type cells (Figures 4E and 4F). Also, variations in migratory behavior

WT   *bmp2b*-MO   *bmp2b*-MO +
Bmp-bead dorsal

A   B   C
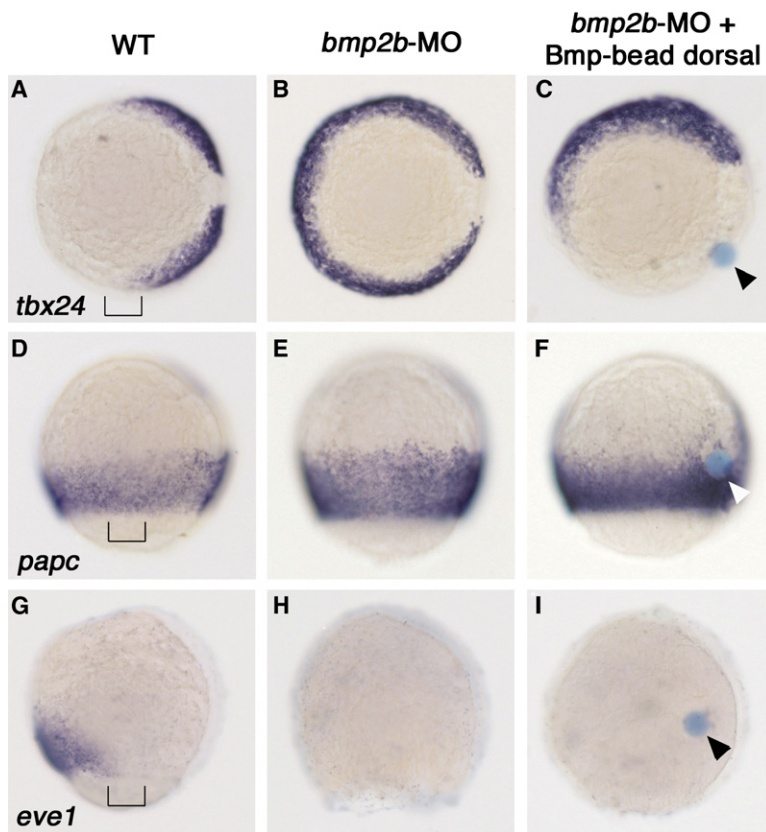
tbx24

D   E   F

papc

G   H   I

eve1

Figure 2. The Bmp Beads Generate a Broad Field of Laterally Specified Mesoderm

Embryos at the 80% epiboly stage, dorsal to the right, after whole-mount in situ hybridizations with probes indicated on the left side of each row, and after treatment indicated on the top of each column. Vegetal view shown in (A)–(C); lateral view shown in (D)–(I), anterior to the top. Bmp beads are indicated with arrowheads. The mesoderm throughout the entire bead-bearing side of the embryos displays absence of *tbx24* and *eve1*, but presence of *papc* [46] transcripts, as is normally characteristic for a narrow lateral domain of wild-type (WT) embryos at 90° from the shield (indicated by brackets in [A], [D], and [G]). Note the presence of *papc*-positive cells in close proximity to the bead in (F), in line with the observation that cell movements become prominent only after mid-gastrula stages.

cannot be explained by differences in the stability of lamellipodia. Thus, in *bmp2b*-overexpressing embryos (reduced cell motility), lamellipodia were even slightly more persistent than in *bmp2b* morphants (high cell motility). Similarly, in wild-type embryos, lamellipodia projecting ventrally (against the migration direction) persisted slightly longer than dorsally projecting lamellipodia, while no dorsal-ventral differences were apparent upon gain or loss of Bmp signaling (Figure 4G).

Nevertheless, we found consistent differences in the rates with which the retraction of lamellipodia was associated with a displacement of the cell body into the direction of lamellipodial projections (see for examples, Figure S3). In wild-type embryos of the 75%–80% epiboly stage, approximately 50% of lamellipodial retractions were accompanied by cellular displacements, and there was no significant directional preference (Figure 4H). At 85%–90% epiboly, however, 80% of the dorsal, but only 20% of the ventral, lamellipodia caused cell displacements (Figure 4I). In contrast, in *bmp2b* morphants we observed high coupling of lamellipodial retraction with cell body movement at both mid and late gastrula stages, and in both dorsal and ventral directions (Figures 4H and 4I), consistent with the cells' zigzagging migration at rather high speed (Figure 4B). Upon *bmp2b* overexpression, however, retractions of both dorsally and ventrally projecting lamellipodia were much less frequently associated with cell body displacements (Figures 4H and 4I), consistent with the slow and undirected cell movements (Figure 4C). These data suggest that Bmp signaling has a negative effect on lamellipodial functionality and their ability to drive cell movements.

Bmp Signaling Negatively Regulates Ca^{2+}/Cadherin-Dependent Cell-Cell Adhesiveness In Vitro and In Vivo

Lamellipodia-driven displacement of cell bodies into the direction of projection requires an attachment of protrusions to the extracellular matrix or to neighboring cells. Confocal time-lapse in vivo imaging of transplanted fluorescently labeled cells revealed that mesodermal cells do form cell-cell contacts via lamellipodia. In the case of *alk8* morphant cells (low Bmp signaling), these contacts were frequently stable, such that cells approached and adhered to each other upon lamellipodial retractions (Figure 5A; n = 7/9 contacting cells in 4 embryos). In contrast, lamellipodia of cells expressing constitutively active Alk8 (CA*alk8*; high Bmp signaling) often just touched neighboring cells transiently, and retracted again without pulling cells toward each other (Figure 5B; n = 7/8 cells in 5 embryos).

To further study the effect of Bmp signaling on cell-cell adhesion, we performed cell aggregation experiments with primary cultures of zebrafish mesodermal cells. Embryos were injected at the 1-cell stage with mesoderm-inducing *cyclops* mRNA [19], a tracer dye, and either *alk8* MO or CA*alk8* mRNA, followed by cell dissociation and culturing at late blastula (sphere) stages. After 4 hr in culture, *alk8* morphant cells formed significantly larger confluent aggregates than CA*alk8*-mRNA cells (Figures 5E, 5F, and 5I). When cultures were incubated overnight, most *alk8* morphant cells ended up in large tight aggregates (appearing transparent) (Figure 5J), whereas CA*alk8*-mRNA cells remained in a looser organization and formed smaller aggregates (Figure 5K). In cocultures of *alk8*-MO and CA*alk8*-mRNA
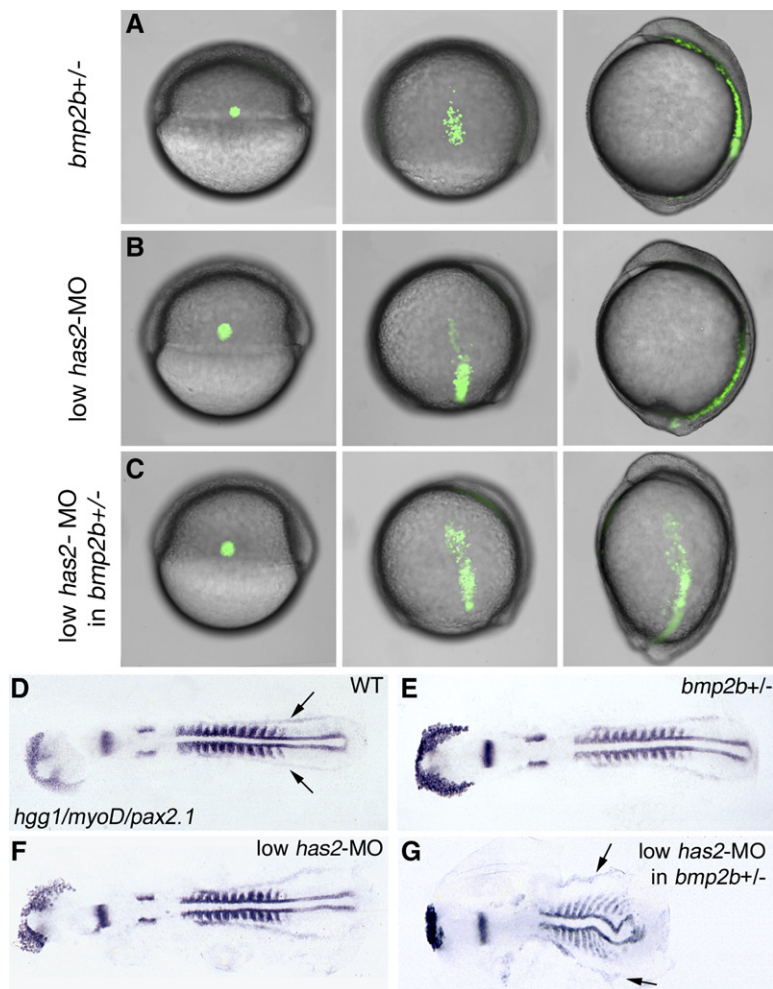
Figure 3. *bmp2b* and *has2* Display Genetic Interaction during Dorsal Convergence, but Not Dorsoventral Patterning

(A–C) Live embryos with fluorescently labeled group of lateral mesodermal cells after treatment indicated on the left side of each row, at the onset, the middle, and the end of gastrulation; lateral views, dorsal to the right, anterior at the top. For wild-type controls, see Figure 1B.

(D–G) Same embryos after whole-mount in situ hybridization at the 12-somite stage with *hgg1*, marking hatching gland precursor cells, *myoD*, marking muscle precursors, and *pax2.1*, marking midbrain-hindbrain boundary, otic placodes, and pronephric ducts. Note that in (G), the *bmp2b* heterozygote injected with low amounts of *has2* MO displays an undulated notochord and laterally expanded somites, resulting from reduced convergence movements, while *pax2.1*-positive pronephric cells (indicated by arrows in [D] and [G]) are present in normal numbers, indicating that the embryo is not dorsalized (compare with [3]).

cells, the more cohesive *alk8*-MO cells usually ended up in the more tightly packed centers of aggregates, while the CA*alk8*-mRNA cells were located in the more loosely packed periphery (Figure 5L). Furthermore, adhesion of *alk8*-MO cells was strongly inhibited by medium addition of EGTA, a chelator of extracellular Ca^{2+}, whereas addition of RGD peptide, an inhibitor of integrin-fibronectin binding [20], had no effect (Figures 5G–5I). Together, this suggests that Bmp signaling has a negative effect on Ca^{2+}-dependent cell-cell adhesion within the mesoderm.

Ca^{2+}-dependent cell adhesiveness is often accomplished by members of the Cadherin family of transmembrane adhesion proteins [21]. To address the involvement of Cadherins in Bmp-regulated stability of mesodermal cell contact points in vivo (see Figure 5A and 5B), we performed time-lapse recordings of fluorescently labeled cells upon combined loss of Bmp signaling (higher adhesiveness) and loss of Cadherin function, or upon combined gain of Bmp signaling (lower adhesiveness) and gain of Cadherin function. Transplanted cells that had been coinjected with *alk8* MO and mRNA encoding nonsecreted dominant-negative Cadherin displayed unstable lamellipodia-cell contacts and failed to approach each other (Figure 5C; n = 6/8 cells in 5 embryos), similar to cells expressing constitutively active Alk8 (CA*alk8*; Figure 5B). This indicates that cell-cell

adhesiveness obtained upon loss of Bmp signaling is Cadherin dependent. In reverse, cells coinjected with CA*alk8* and *ncad* (*chd2*) mRNA displayed high stability of lamellipodia-cell contact points and cell displacements (Figure 5D; n = 7/8 cells in 6 embryos), comparable to cells upon loss of Bmp signaling (Figure 5A). This indicates that gain of Cadherin function can rescue the migratory defects caused by increased Bmp signaling levels, suggesting that Cadherin-dependent cell adhesiveness is epistatic to and negatively regulated by Bmp signaling.

Genetic Interaction of N-Cadherin and Bmp Signaling during Dorsal Convergence, but Not during Dorsoventral Patterning

Further support for an interplay of Bmp signaling and Cadherins in Bmp-guided convergence movements was obtained via Bmp-Cadherin synergistic enhancement studies, now combining gain of Bmp signaling (lower adhesiveness) with loss of Cadherin function and vice versa. In two independent enhancer screens of the *chordin* mutation *din*[tt250] [22] (higher Bmp signaling) [23] (see Supplemental Data), we isolated *n-cadherin* (*cdh2*) loss-of-function mutations exacerbating the overall morphology in double mutant embryos at 24 hpf (Figures 6A–6D and Figure S4). Whereas convergence was normal in *cdh2* morphants (Figure 6F; n = 7/7)
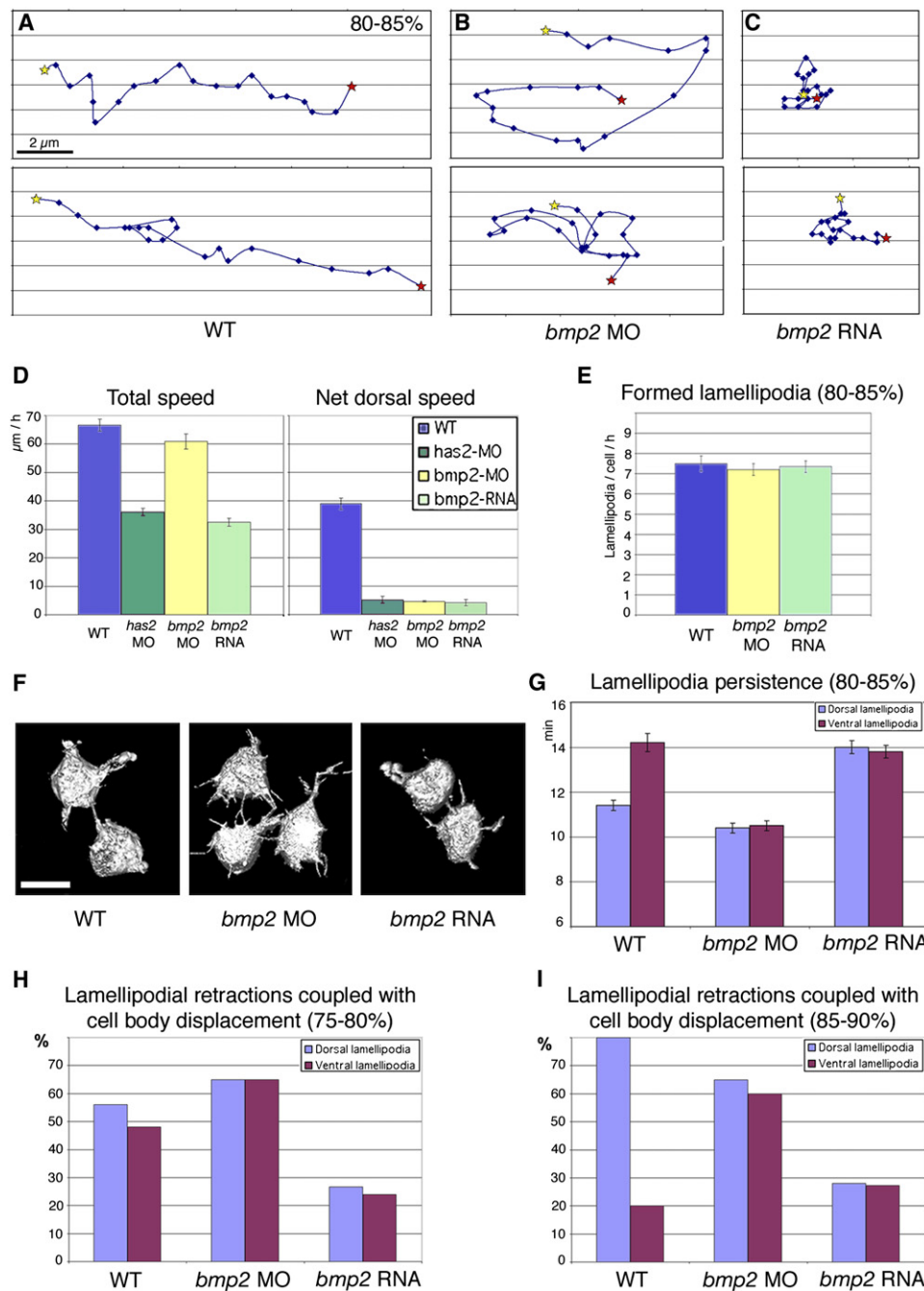
Figure 4. Bmp Signaling Affects the Directionality of Cell Migration and the Functionality of Lamellipodia, but Not Lamellipodia Formation Per Se

(A–C) Representative examples of time-lapse recordings of individual lateral mesodermal cells over 20 min with 1 min intervals (80%–85% epiboly stage). Dorsal is to the right, animal pole to the top; the start and end points are indicated by yellow and red asterisks, respectively.

(D) Graphical illustrations of the total speed and the net dorsal speed of lateral mesodermal cells (in μm/hr; n = 20) in wild-type, *has2* morphant, *bmp2b* morphant, and *bmp2b*-overexpressing embryos, calculated from time-lapse recordings as shown in (A)–(C). Error bars indicate standard errors, calculated by Excel software.

(E) Newly formed lamellipodia per cell and hour in wild-type, *bmp2b* morphant, and *bmp2b*-overexpressing embryos from 80%–85% epiboly. Error bars indicate standard errors, calculated by Excel software.

(F) 3D confocal reconstructions of individual mGFP-labeled lateral mesodermal cells at 85% epiboly stage; dorsal to the right. All cells form multiple lamellipodia, which project into random directions. Scale bar represents 10 μm.

(G) Persistence (time between outgrowth and retraction in minutes) of dorsally (in blue) and ventrally (in red) projecting lamellipodia in embryos between 80% and 85% epiboly. Error bars indicate standard errors, calculated by Excel software.

(H and I) Percentages of lamellipodia of mesodermal cells at 90° from the dorsal shield, for which lamellipodial retraction was coupled with a displacement of the cell body by at least half a cell diameter into the direction of their projection. Comparison of dorsally (in blue) and ventrally projecting (in red) lamellipodia in embryos between 75% and 80% epiboly (H) and between 85% and 90% epiboly (I). For every condition/column, 20–25 lamellipodia from 4–6 independent experiments were scored. See Figure S3 for examples. WT, wild-type; MO, *bmp2b* morphant; RNA, *bmp2b*-overexpressing. The data in (D), (E), and (G) are presented as mean ± SEM.

and only moderately compromised in *chordin* morphants (Figure 6I; n = 6/6), *cdh2/chordin* double morphants displayed significantly stronger convergence defects (Figure 6J; n = 7/8). However, shifts in dorsoventral patterning of *cdh2/chordin* double morphants were not more severe than in *chordin* single morphants (Figures 6G, 6H, 6K, and 6L and Figures S2B and S2D). This indicates that loss of N-cadherin synergistically enhances the convergence defects of *chordin* morphants without affecting differential dorsoventral cell-fate specification. Consistent results were obtained when partial loss of Bmp signaling was combined with gain of N-cadherin function. *bmp2b* heterozygotes injected with *cdh2* mRNA displayed strong convergence defects (Figure 6N; n = 4/4) similar to those of *bmp2b* morphants (Figure 1F), although convergence was normal in uninjected *bmp2b* heterozygotes (Figure 3A; n = 4/4) and in wild-type siblings injected with the same amounts of *cdh2* mRNA (Figure 6M; n = 6/6). Together, these results indicate that the effect of Bmp signaling on migration guidance of lateral mesodermal cells depends on Cadherin levels.

Locally Applied Ca²⁺-Chelators Can Replace Bmp Beads to Restore Directed Cell Migration in *bmp2b* Morphants

With a negative effect of Bmp signaling on cell-cell adhesion, it is tempting to speculate that the ventral-to-dorsal Bmp gradient drives convergence movements by generating a reverse dorsal-to-ventral gradient of Ca^{2+}-dependent cell adhesiveness. Accordingly, the convergence defects of *bmp2b* morphant embryos should be due to homogeneously high adhesiveness of mesodermal cells along the entire dorsoventral axis. To test this notion, we locally applied extracellular Ca^{2+} chelators into *bmp2b* morphant embryos. Cadherins have multiple Ca^{2+} binding sites, and according to structural studies, their conformation and ability to undergo trans-oligomerization strictly depend on Ca^{2+} concentrations [24, 25]. Therefore, we reasoned that a Ca^{2+} gradient might restore the postulated gradient of adhesiveness and convergence movements. Indeed, when implanting BAPTA beads into ventral or dorsal positions, lateral cells moved away from the beads, as described above upon implantation of Bmp beads (Figures 7A and 7B; n = 9/9). Similarly, injections of small drops of EGTA (0.5 nl, 5 mM) into dorsal regions of *bmp2b* morphants induced ventral movement of lateral cells (Figure 7C; n = 4/5). However, in contrast to Bmp beads (Figure 1L; Figure S1C), BAPTA beads also induced cell migration when implanted into *alk8* or *smad5* morphant embryos (Figure 7D; n = 5/6; and data not shown, n = 5/5). Also, contrary to Bmp beads (Figure 2), the Ca^{2+} chelators did not influence Bmp signaling or dorsoventral patterning, as revealed by the coexpression of *papc* (n = 7/7) and *tbx24* (n = 11/11) around the bead and the absence of antiphosphorylated Smad1/5/8 immunostaining (n = 10/10) (Figures 7E and 7F; and data not shown). Together, this indicates that a reverse Ca^{2+}-dependent cell adhesion gradient is at play downstream of the Bmp gradient to direct convergence movements without affecting Bmp-dependent differential dorsoventral cell-fate specification.

Discussion

While most studies of Bmps are concerned with their roles to regulate cell-fate determination and differentiation, there have been a number of reports describing effects on cell or axon guidance. For instance, Bmp7/Gdf7 heterodimers from the roof plate have been shown to act as a repellent to establish ventral trajectories of commissures [26]. Similarly, Bmp4 has been shown to block lung endoderm migration and bud outgrowth during lung bud morphogenesis [27]. However, the mechanisms underlying these repulsive effects have remained elusive. Here, we show that lateral mesodermal cells of the gastrulating zebrafish embryo also migrate away from the source of Bmps (Figure 1H). Classical chemokines usually act by posttranslational modifications of the cytoskeleton (see for review [28]). In contrast, Bmp signaling appears to determine migration direction in a more indirect mode. Thus, the Bmp signals do not have to be received by the migrating lateral mesodermal cells themselves (Figures 1K and 1L). Rather, it is the Bmp gradient in the environment that is required to guide cells. In addition, Bmp signaling requires its downstream transcription factor Smad5 (Figure S1).

Smad5-mediated transcriptional regulation by Bmp signaling plays a crucial role during differential cell-fate determination along the dorsoventral axis of the zebrafish embryo (see for review [10]). However, several of our data indicate that the effect of Bmps on convergence movements is independent of their patterning function. Thus, implanted Bmp beads induce cell migration without restoring the whole spectrum of dorsoventral cell fates (Figure 2). Furthermore, in a *has2* hypomorphic background, partial loss of Bmp signaling leads to severe convergence and extension defects without corresponding shifts in dorsoventral patterning (Figure 3). This genetic interaction with Has2 indicates that lamellipodia play a crucial role during Bmp-guided cell movements. Finally, we found a similar convergence-specific genetic interaction between Bmp signaling and the cell adhesion molecule N-cadherin (Figure 6), in line with the notion that Bmps guide convergence by regulating cell adhesiveness (see below).

In the past years, several regulators of convergence and extension movements have been identified, such as components of the noncanonical Wnt signaling (see for recent review [2]). Strikingly, Wnt5a and Wnt11 have been shown to regulate Ca^{2+}-dependent cell adhesiveness of mesodermal cells [29, 30], as reported here for Bmps. Furthermore, the *wnt11* and *wnt5a* expression domain have been shown to be expanded in *bmp2b* and reduced in *chordin* mutants [5]. In this light, one could imagine that Bmp signaling guides convergence movements via transcriptional regulation of convergence and extension regulators like Wnt11. However, we found that Bmp beads can induce ventral movements of lateral cells even in the absence of Wnt5 and Wnt11 (Figure S1), indicating that the Bmp gradient can guide cell migration independently of noncanonical Wnt signaling. This is consistent with the recent finding that convergence of mesodermal cells in ventrolateral positions is normal in mutants defective in noncanonical Wnt signaling [2, 6]. Similarly, Bmp beads are effective when Fgf signaling is blocked by SU5402 treatment, ruling out that Bmps
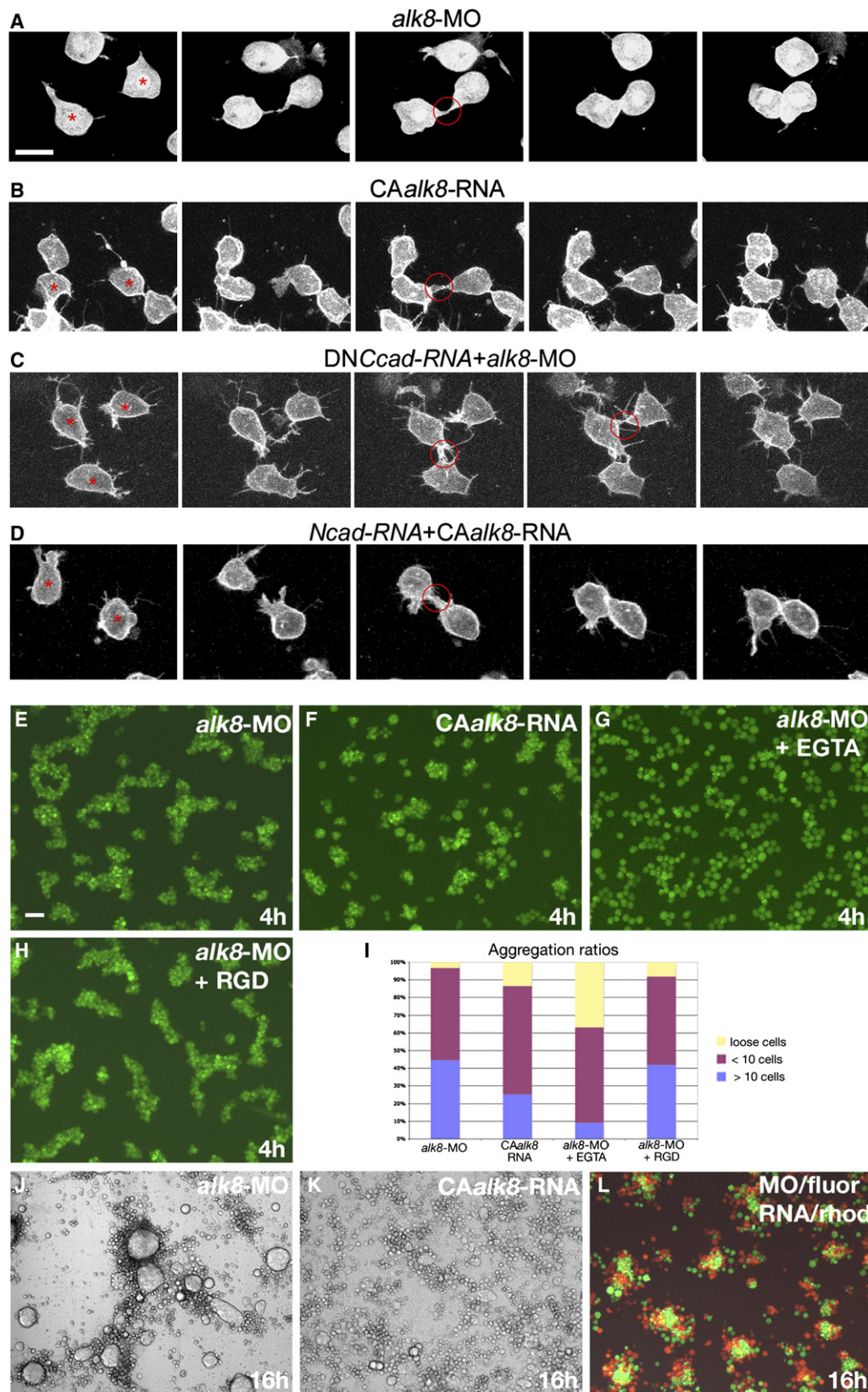
Figure 5. Bmp Signaling Has a Negative Effect on Cadherin-Dependent Stability of Lamellipodia-Mediated Cell-Cell Contacts In Vivo and on Cell-Cell Adhesion of Mesodermal Cells In Vitro

(A–D) Confocal time-lapse recordings of mGFP-labeled lateral mesodermal cells in embryos between 85% and 90% stage. Shown are (A) *alk8* morphant cells/embryo; (B) cells/embryo injected with CA*alk8*-mRNA; (C) *alk8* morphant cells expressing nonsecreted dominant-negative

act via transcriptional regulation of Fgfs and their target genes such as Sprouty2, which in *Xenopus laevis* has been shown to inhibit convergence and extension movements without affecting mesodermal patterning [31].

However, like such other convergence and extension regulators, Bmps appear to act at least in part by regulating Cadherin-dependent cell adhesiveness. Thus, cultured zebrafish mesodermal cells in the absence of Bmp signaling (as on the dorsal side) aggregate better than in the presence of Bmp signaling (as on the ventral side). Accordingly, in vivo imaging of labeled lateral mesodermal cells revealed that attachments through lamellipodia are more stable when Bmp signaling is blocked, an effect that is dependent on Cadherins (Figure 5). Furthermore, *chordin* morphants (higher Bmp signaling) show a strong genetic interaction with morphants in N-cadherin, while gain of N-cadherin leads to a synergistic enhancement of the convergence defects of *bmp2b* heterozygotes (reduced Bmp signaling) (Figure 6). And finally, the effect of Bmp beads to induce emigration of lateral mesodermal cells can be mimicked by implantation of beads loaded with extracellular Ca^{2+} chelators (Figure 7). While we cannot rule out that the latter effects are due to interferences with other Ca^{2+}-dependent proteins in addition to Cadherins, our data in sum suggest that the Bmp gradient generates and acts via a reverse gradient of Ca-dependent cell adhesiveness, which increases from ventral to dorsal regions. We propose that directed cell migration underlying convergence of lateral mesodermal cells occurs in the following mode. Independent of Bmp signaling, cells protrude and retract lamellipodia. Protrusions initially occur in random directions and come in contact with both ventrally and dorsally located cells. Yet, dorsal cells are more adhesive, and therefore lamellipodial attachments to dorsal cells are stronger. Accordingly, they have a higher likelihood to remain stable during lamellipodial retraction, in which case the protrusion-bearing cell will be displaced dorsally. It even is possible that a strong attachment triggers lamellipodial retraction, which would explain why in the absence of Bmp signaling, lamellipodia persist for a slightly shorter time (Figure 4G). To allow further cell migration, even strong cell attachments need to be broken and rebuilt after successful cell pulling. This dynamics in adhesiveness might be achieved via Cadherin endocytosis, as described for E-cadherin (Cdh1) during the anterior-wards migration of prechordal plate cells [30]. In net, such a dynamic behavior will lead to a preferential displacement of lateral cells into dorsal regions where Bmp signaling is lower and Cadherin-dependent adhesiveness is higher.

Our observations also provide a mechanism via which the Bmp gradient can coordinate differential convergence and extension movements along the dorsoventral axis of the zebrafish gastrula [5]. In ventral-most regions, the no-convergence-no-extension zone, highest Bmp signaling levels lead to cell adhesiveness levels below a certain threshold, thereby suppressing both convergence and extension. In ventrolateral regions, however, where Bmp signaling has dropped and cell adhesiveness has risen, the gradient of Bmp signaling results in the reverse adhesiveness gradient, thus accounting for dorsally directed convergence movements of increasing speed.

A similar role of asymmetrically distributed Cdh1 has recently been reported for the directed radial intercalation movements of ectodermal cells during zebrafish epiboly [32, 33]. It was shown that *cdh1* transcripts form a gradient within the ectoderm, with increasing levels toward superficial layers [32]. Whereas in wild-type embryos, radial cell intercalation occurs only from deeper to superficial layers, it is bidirectional in *cdh1* mutants, resulting in a lack of net displacement, comparable to the undirected migratory behavior of lateral mesodermal cells in *bmp2b* morphants (Figure 4B). In addition to epiboly, *cdh1* mutants also display convergence and extension defects [33, 34]. However, *cdh1* does not seem to be the transcriptional Bmp/Smad5 target mediating its effect on convergence guidance. Thus, we failed to detect any dorsoventral differences in the abundance or distribution of *cdh1* mRNA or protein (unpublished data). Similarly, N-cadherin (Cdh2) can most likely be ruled out as the Bmp target, as well as Protocadherin c (Papc), which in *Xenopus* is required for convergence extension movement directionality [35], and which mediates morphogenesis in the dorsal mesoderm by regulating C-cadherin adhesion activity [36]. Thus, zebrafish *cdh2* and *papc*, although displaying preferential expression in the mesoderm, are not expressed in a graded fashion and are insensitive to alterations in Bmp signaling. Furthermore, zebrafish *cdh2* mutants and *papc* morphants show only very minor, if any, convergence defects (Figure 6; and unpublished data). Nevertheless, our genetic interaction studies (Figure 6) indicate that the Bmp target must encode a protein closely cooperating with N-cadherin or modulating Cadherin function.

This Bmp-regulated gradient of cell adhesiveness is particularly important in ventrolateral regions of the embryo. In more dorsal regions, control of convergence might progressively be taken over by other factors, such as noncanonical Wnt signals and the postulated chemoattractant from the dorsal midline [6, 9]. Interestingly, in

---

C-Cadherin after transplantation in *alk8* morphant host; and (D) cells coinjected with CA*alk8* and *ncad* mRNA after transplantation in CA*alk8* mRNA-injected host. The two cells indicated with asterisks in the first photos of (A)–(D) form lamellipodia that contact each other. In (A) and (D), this contact point is stable, and cell bodies are displaced toward each other, while in (B) and (C), it is only transient, and cells remain in distance. Average direct contact durations (in min) and spatial approaches of cells during lamellipodia retractions (in μm) were: (A) >13.3 min, 9.4 ± 4.1 μm, n = 9; (B) 2.5 ± 1.6 min, 1.5 ± 0.5 μm, n = 8; (C) 5.5 ± 1.9 min, 1.3 ± 0.5 μm, n = 6; (D) >15.5 min, 11.1 ± 2.8 μm, n = 8. For (A) and (D), most cell contacts still existed at the end of the time-lapse recordings. Scale bar represents 10 μm.
(E–H and J–L) Primary cultures of mesoderm progenitor cells labeled with fluorescein or rhodamin dextran and plated on fibronectin, after 4 hr (E–H) or overnight (J–L) incubation. Scale bar in (E) represents 100 μm. Embryos had been injected with *alk8*-MO (E, G, H, J, and L) or CA*alk8*-mRNA (F, K, and L). (G and H) Medium supplemented with EGTA (G) or RGD (H). Aggregation of *alk8*-MO cells is strongly inhibited by a reduction of extracellular Ca^{2+} levels but is independent of integrin-fibronectin binding.
(I) Ratios of loose (yellow), small (≤10 cells; red), and large (>10 cells; blue) aggregates in *alk8*-MO, CA*alk8*-mRNA, *alk8*-MO + EGTA, and *alk8*-MO + RGD cultures after 4 hr. Cells numbers in aggregates were determined at higher magnification as described elsewhere [30].
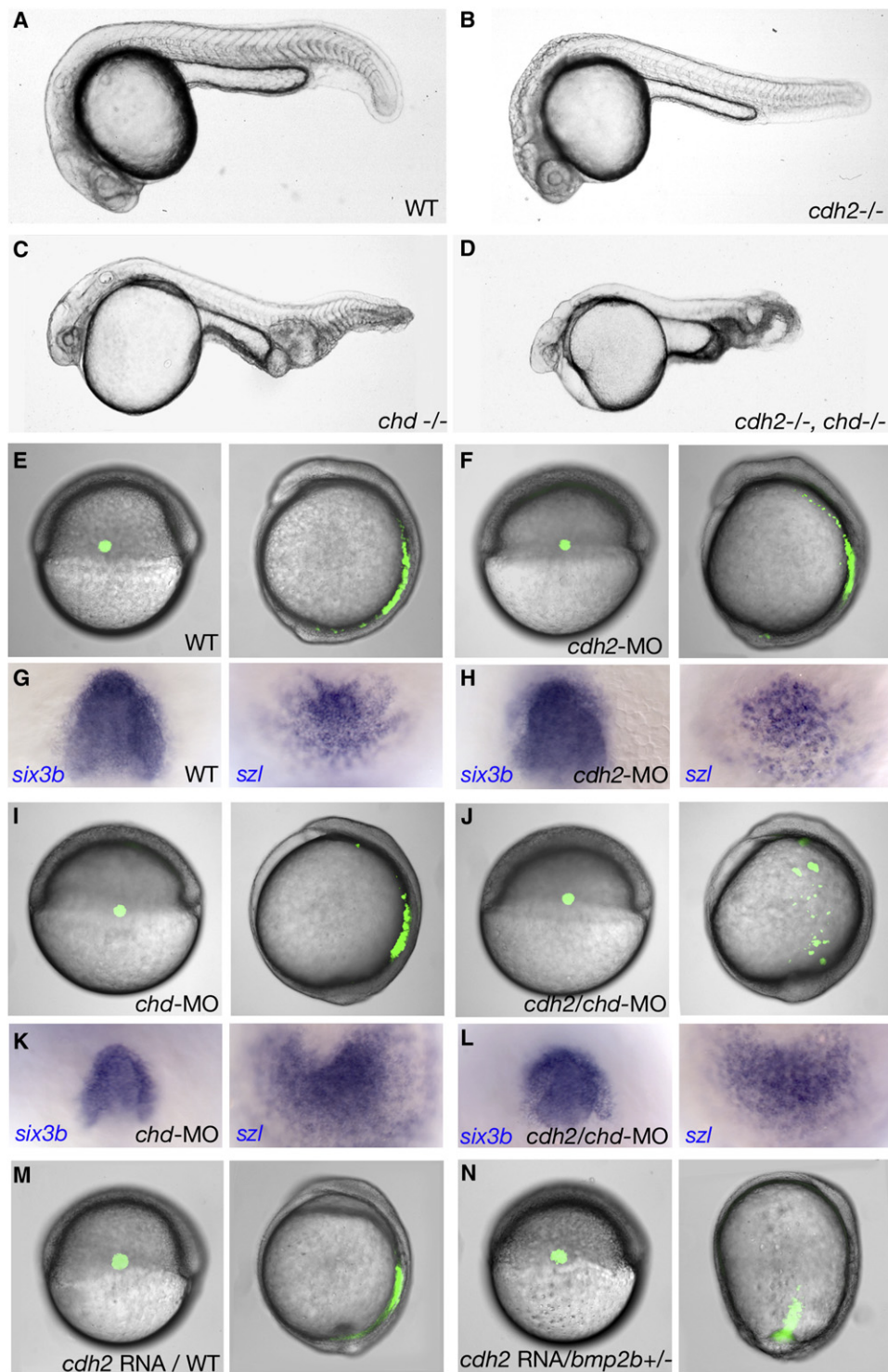
Figure 6. Defects in Convergence, but Not in Dorsoventral Patterning, Are Synergistically Enhanced upon Combined Loss of Chordin and N-Cadherin and in *bmp2b* Heterozygotes after Moderate *n-cadherin* Overexpression

(A–D) Lateral overviews of live embryos of indicated genotype at 24 hpf (*cdh2* allele *pac^{fr7}*; *chd* allele *din^{tt250}*)

(E, F, I, J, M, N) Live embryos with fluorescently labeled mesoderm cells at the onset and end of gastrulation. Coinjection of small amounts of *cdh2*-MO and *chd*-MO in wild-type embryos (J) or injection of small amounts of *cdh2*-mRNA in *bmp2b^{+/−}* embryos (N) lead to a synergistic enhancement of the defects in convergence movements.

(G, H, K, L) Same embryos as shown in (E), (F), (I), (J), at 5-somite stage and after in situ hybridizations for *six3b* (left, animal views), a marker for anterior neuroectoderm, and *szl* (right, vegetal views), a marker for posterior mesoderm. The *chd/cdh2* double morphant (L) displays a *six3b* expression domain not smaller than that of the *chd* single morphant (K), and a *szl* domain not larger than that of the *chd* morphant, indicating that the ventralization caused by loss of Chd is not further enhanced by the simultaneous loss of Cdh2.
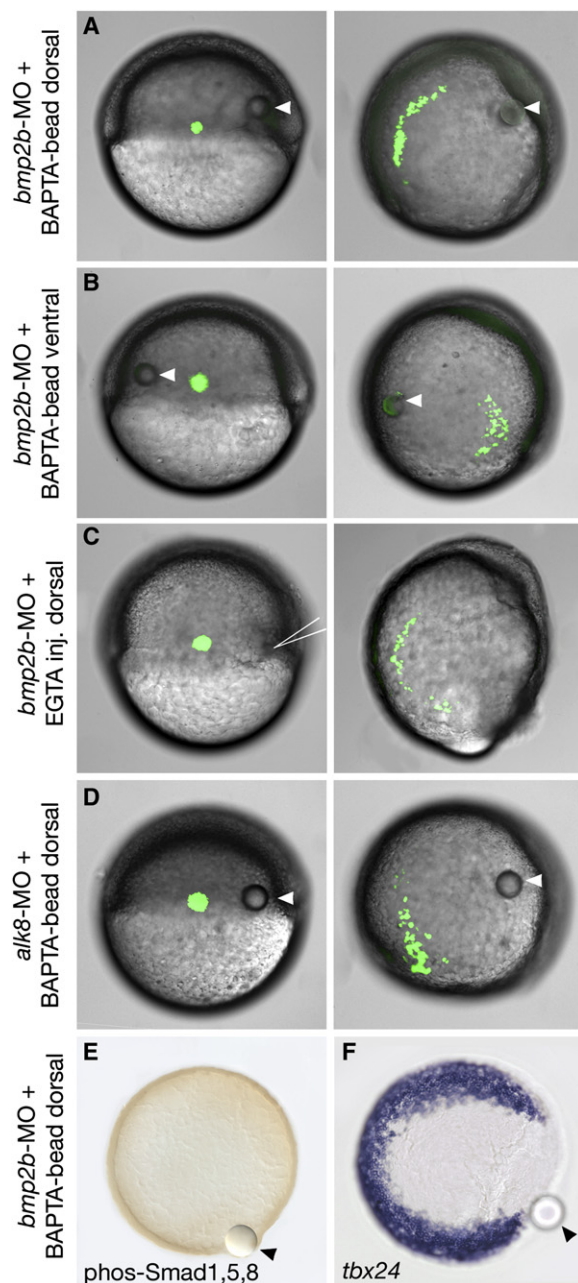
Figure 7. Locally Applied Ca²⁺ Chelators Induce Movement of Lateral Mesodermal Cells in an Alk8-Independent Fashion and without Affecting Dorsoventral Patterning

(A)–(D) Live embryos with a fluorescently labeled group of lateral mesodermal cells at the onset of gastrulation (shield) and at a late gastrula stage (90% epiboly).

(A, E, and F) *bmp2b* morphants with dorsolateral BAPTA beads.

(B) *bmp2b* morphant with ventrolateral BAPTA bead.

(C) *bmp2b* morphant after dorsolateral injection of EGTA (arrow).

(D) *alk8* morphant with dorsolateral BAPTA bead.

(E and F) Vegetal views of embryos at 80% epiboly stage; (E) anti-phos Smad1/5/8 immunostaining; (F) *tbx24* in situ hybridization. Implanted beads are indicated by arrowheads.

Xenopus embryos, the Tgfβ family member Activin, which is involved in antero-posterior patterning of the dorsal axis, has been shown to determine the direction of tissue elongation in the chordamesoderm during convergent extension [37]. It acts in parallel to the noncanonical Wnt signaling pathways, similarly to the Wnt5/11-independent role of Bmps in the lateral mesoderm described here. Also, Activin has been shown to regulate C-cadherin-dependent cell-cell adhesiveness, without any apparent changes in Cadherin protein levels or distribution [38], similar to what we observed for Bmps. Thus, similar mechanisms involving different members of the same family of growth factors might be at play ventrally and dorsally to link morphogenetic movements with patterning and differential cell fate determination.

Experimental Procedures

Fish Strains and Genotyping

Mutant lines used were *swr*[ta72] (*bmp2b*; [39, 40]), *dino*[tt250] (*chordin*; [22]), *pac*[fr7], *pac*[vu91], and *pac*[vu125] (*N-cadherin/cdh2*; [23]; and Supplemental Data). Genotyping was carried out as described in the Supplemental Data.

Morpholino Oligonucleotides and mRNA Injections

Morpholino oligonucleotides (MOs) were purchased from Gene Tools and injected as described previously [41]. Sequences, injected amounts, and references are given in the Supplemental Data. Synthetic mRNA of *bmp2b* (3 ng/μl together with 0.12 mM *chordin*-MO), membrane-bound GFP (mGFP) [42], *cyclops* [30], constitutively active *alk8* (CA*alk8*) [11], C-terminally truncated *Xenopus* C-cadherin [43] (100 ng/μl), and mouse *Ncad* (50 ng/μl for Figure 5; 25 ng/μl for Figure 6) was made from pCS2+ constructs with the Message Machine-Kit (Ambion).

Whole-Mount In Situ Hybridization and Immunohistochemistry

In situ hybridization and antibody stainings were carried out as previously described [44]. References for the cDNAs used for riboprobe synthesis are given in the Supplemental Data. Phosphorylated Smad 1,5,8 antibody (Cell Signaling) was applied at 1:200 and detected with the Vectastain ABC Kit (Vector Laboratories).

Bead Implantations and Uncaging Experiments

Agarose beads (Affigel blue, BioRad) [45] were rinsed twice in PBS and incubated for 1 hr at 37°C with 100 ng/μL recombinant human BMP4 and BMP7 (R&D Systems) or with 100 ng/μl BSA as control. BAPTA-polystyrene beads (Calcium Sponge S, Molecular Probes) were used to bind extracellular calcium. Beads were implanted close to the margin at shield stage with a fine Tungsten needle and forceps. Fluorescent labeling via uncaging of DMNB-caged fluorescein (Molecular Probes) and imaging of mesendoderm cells was carried out as described previously [3].

Time-Lapse Imaging and Image Analysis

Lateral mesodermal cells were photographed at 40× magnification with Nomarski optics with a Zeiss Axioplan2 microscope and an ORCA ER C4742-95 camera (Hamamatsu). Recordings were analyzed with the Openlab (Improvision) and Microsoft Excel software. Confocal imaging was performed with a Zeiss LSM510 META microscope, acquiring stacks every 2 min.

Cell Transplantations

In order to visualize cellular processes, 5–10 lateral marginal cells of donor embryos injected with *mGFP*-mRNA and *bmp2b*-mRNA, *bmp2b*-MO, or water, were transplanted at the shield stage into the same region of unlabeled hosts of the same genotype. For cell-autonomy studies, donors were injected with *bmp2b*-MO and fluorescein dextran (Molecular Probes) or with *alk8*-MO and rhodamin dextran (Molecular Probes), while recipient embryos were injected with *bmp2b*-MO or *alk8*-MO only. At the shield stage, Bmp beads were implanted into the dorsolateral marginal zone of recipients, followed by transplantation of lateral marginal cells of the two different donor types ventral of the beads.

Cell Culture

Primary zebrafish mesodermal cell cultures were performed essentially as described [16], after coinjection of *cyclops* mRNA, *alk8* MO or CA*alk8* mRNA, and Rhodamin- or Fluorescein dextran at the 1-cell stage. 10–20 dechorionated embryos were dissociated at the sphere stage with 1 ml Accutase (eBioscience). Cell pellets were taken up in Leibrovitz medium (L15, GIBCO), containing 100 U/ml penicillin and 100 μg/mL streptomycin, and plated on fibronectin-coated 96-well plates at a density of 6 embryos/well. For inhibitor experiments, 5 mM EGTA [30] or 250 μM RGD [19] were added to the L15-medium.

Supplemental Data

Supplemental Data include four figures and Experimental Procedures and can be found with this article online at http://www.current-biology.com/cgi/content/full/17/6/475/DC1/.

References

1. Warga, R.M., and Kimmel, C.B. (1990). Cell movements during epiboly and gastrulation in zebrafish. Development *108*, 569–580.
2. Solnica-Krezel, L. (2006). Gastrulation in zebrafish—all just about adhesion? Curr. Opin. Genet. Dev. *16*, 1–9.
3. Bakkers, J., Kramer, C., Pothof, J., Quaedvlieg, N.E., Spaink, H.P., and Hammerschmidt, M. (2004). Has2 is required upstream of Rac1 to govern dorsal migration of lateral cells during zebrafish gastrulation. Development *131*, 525–537.
4. Sepich, D.S., Myers, D.C., Short, R., Topczewski, J., Marlow, F., and Solnica-Krezel, L. (2000). Role of the zebrafish *trilobite* locus in gastrulation movements of convergence and extension. Genesis *27*, 159–173.
5. Myers, D.C., Sepich, D.S., and Solnica-Krezel, L. (2002). Bmp activity gradient regulates convergent extension during zebrafish gastrulation. Dev. Biol. *243*, 81–98.
6. Sepich, D.S., Calmelet, C., Kiskowski, M., and Solnica-Krezel, L. (2005). Initiation of convergence and extension movements of lateral mesoderm during zebrafish gastrulation. Dev. Dyn. *234*, 279–292.
7. Yamashita, S., Miyagi, C., Carmany-Rampey, A., Shimizu, T., Fujii, R., Schier, A.F., and Hirano, T. (2002). Stat3 controls cell movements during zebrafish gastrulation. Dev. Cell *2*, 363–375.
8. Miyagi, C., Yamashita, S., Ohba, Y., Yoshizaki, H., Matsuda, M., and Hirano, T. (2004). STAT3 non cell-autonomously controls planar cell polarity during zebrafish convergence and extension. J. Cell Biol. *166*, 975–981.
9. Lin, F., Sepich, D.S., Chen, S., Topczewski, J., Yin, C., Solnica-Krezel, L., and Hamm, H. (2005). Essential role of Gα12/13 in distinct cell behaviors driving zebrafish convergence and extension gastrulation movements. J. Cell Biol. *169*, 777–787.
10. Hammerschmidt, M., and Mullins, M.C. (2002). Dorsoventral patterning in the zebrafish: bone morphogenetic proteins and beyond. Results Probl. Cell Differ. *40*, 72–95.
11. Bauer, H., Lele, Z., Rauch, G.J., Geisler, R., and Hammerschmidt, M. (2001). The type I serine/threonine kinase receptor Alk8/Lost-a-fin is required for Bmp2b/7 signal transduction during dorsoventral patterning of the zebrafish embryo. Development *128*, 849–858.
12. Mintzer, K.A., Lee, M.A., Runke, G., Trout, J., Whitman, M., and Mullins, M.C. (2001). *lost-a-fin* encodes a type I BMP receptor, Alk8, acting maternally and zygotically in dorsoventral pattern formation. Development *128*, 859–869.
13. Hild, M., Dick, A., Rauch, G.J., Meier, A., Bouwmeester, T., Haffter, P., and Hammerschmidt, M. (1999). The *smad5* mutation *somitabun* blocks Bmp2b signaling during early dorsoventral patterning of the zebrafish embryo. Development *126*, 2149–2159.
14. Mohammadi, M., McMahon, G., Sun, L., Tang, C., Hirth, P., Yeh, B.K., Hubbard, S.R., and Schlessinger, J. (1997). Structures of the tyrosine kinase domain of fibroblast growth factor receptor in complex with inhibitors. Science *276*, 955–960.
15. Fuhrmann, G., Leisser, C., Rosenberger, G., Grusch, M., Huettenbrenner, S., Halama, T., Mosberger, I., Sasgary, S., Cerni, C., and Krupitza, G. (2001). Cdc25A phosphatase suppresses apoptosis induced by serum deprivation. Oncogene *20*, 4542–4553.
16. Montero, J.A., Kilian, B., Chan, J., Bayliss, P.E., and Heisenberg, C.P. (2003). Phosphoinositide 3-kinase is required for process outgrowth and cell polarization of gastrulating mesendodermal cells. Curr. Biol. *13*, 1279–1289.
17. Joly, J.S., Joly, C., Schulte-Merker, S., Boulekbache, H., and Condamine, H. (1993). The ventral and posterior expression of the zebrafish homeobox gene *eve1* is perturbed in dorsalized and mutant embryos. Development *119*, 1261–1275.
18. Nikaido, M., Kawakami, A., Sawada, A., Furutani-Seiki, M., Takeda, H., and Araki, K. (2002). *Tbx24*, encoding a T-box protein, is mutated in the zebrafish somite-segmentation mutant *fused somites*. Nat. Genet. *31*, 195–199.
19. Puech, P.H., Taubenberger, A., Ulrich, F., Krieg, M., Muller, D.J., and Heisenberg, C.P. (2005). Measuring cell adhesion forces of primary gastrulating cells from zebrafish using atomic force microscopy. J. Cell Sci. *118*, 4199–4206.
20. Ruoslahti, E., and Pierschbacher, M.D. (1987). New perspectives in cell adhesion: RGD and integrins. Science *238*, 491–497.
21. Wheelock, M.J., and Johnson, A.L. (2003). Cadherins as modulators of cellular phenotype. Annu. Rev. Cell Dev. Biol. *19*, 207–235.
22. Schulte-Merker, S., Lee, L.J., McMahon, A.P., and Hammerschmidt, M. (1997). The zebrafish organizer requires *chordino*. Nature *387*, 862–863.
23. Lele, Z., Folchert, A., Concha, M., Rauch, G.J., Geisler, R., Rosa, F., Wilson, S.W., Hammerschmidt, M., and Bally-Cuif, L. (2002). *parachute/n-cadherin* is required for morphogenesis and maintained integrity of the zebrafish neural tube. Development *129*, 3281–3294.
24. Haussinger, D., Ahrens, T., Sass, H.J., Pertz, O., Engel, J., and Grzesiek, S. (2002). Calcium-dependent homoassociation of E-cadherin by NMR spectroscopy: changes in mobility, conformation and mapping of contact regions. J. Mol. Biol. *324*, 823–839.
25. Pertz, O., Bozic, D., Koch, A.W., Fauser, C., Brancaccio, A., and Engel, J. (1999). A new crystal structure, Ca2+ dependence and mutational analysis reveal molecular details of E-cadherin homoassociation. EMBO J. *18*, 1738–1747.
26. Butler, S.J., and Dodd, J. (2003). A role for BMP heterodimers in roof plate-mediated repulsion of commissural axons. Neuron *38*, 389–401.
27. Weaver, M., Dunn, N.R., and Hogan, B.L.M. (2000). Bmp4 and Fgf10 play opposing roles during lung bud morphogenesis. Development *127*, 2695–2704.
28. Dormann, D., and Weijer, C.J. (2006). Chemotactic cell movement during *Dictyostelium* development and gastrulation. Curr. Opin. Genet. Dev. *16*, 367–373.
29. Torres, M.A., Yang-Snyder, J.A., Pucell, S.M., DeMarais, A.A., McGrew, L.L., and Moon, R.T. (1996). Activities of the Wnt-1 class of secreted signaling factors are antagonized by the Wnt-5A class and by a dominant negative cadherin in early I development. J. Cell Biol. *133*, 1123–1137.
30. Ulrich, F., Krieg, M., Schötz, E.-M., Link, V., Castanon, I., Schnabel, V., Taubenberger, A., Mueller, C., Puech, P.-H., and Heisenberg, C.-P. (2005). Wnt11 functions in gastrulation by controlling cell cohesion through Rab5c and E-cadherin. Dev. Cell *9*, 555–564.

31. Nutt, S.L., Dingwell, K.S., Holt, C.E., and Amaya, E. (2001). *Xenopus* Sprouty2 inhibits FGF-mediated gastrulation movements but does not affect mesoderm induction and patterning. Genes Dev. *15*, 1152–1166.

32. Kane, D.A., McFarland, K.N., and Warga, R.M. (2005). Mutations in *half baked*/E-cadherin block cell behaviors that are necessary for teleost epiboly. Development *132*, 1105–1116.

33. Shimizu, T., Yabe, T., Muraoka, O., Yonemura, S., Aramaki, S., Hatta, K., Bae, Y.K., Nojima, H., and Hibi, M. (2005). E-cadherin is required for gastrulation cell movements in zebrafish. Mech. Dev. *122*, 747–763.

34. McFarland, K.N., Warga, R.M., and Kane, D.A. (2005). Genetic locus *half baked* is necessary for morphogenesis of the ectoderm. Dev. Dyn. *233*, 390–406.

35. Unterseher, F., Hefele, J.A., Giehl, K., De Robertis, E.M., Wedlich, D., and Schambony, A. (2004). Paraxial protocadherin coordinates cell polarity during convergent extension via RhoA and JNK. EMBO J. *23*, 3259–3269.

36. Chen, X., and Gumbiner, B.M. (2006). Paraxial protocadherin mediates cell sorting and tissue morphogenesis by regulating C-cadherin activity. J. Cell Biol. *174*, 301–311.

37. Ninomiya, H., Elison, R.P., and Winklbauer, R. (2004). Anteroposterior tissue polarity links mesoderm convergent extension to axial patterning. Nature *430*, 364–367.

38. Brieher, W.M., and Gumbiner, B.M. (1994). Regulation of C-cadherin function during activin induced morphogenesis of *Xenopus* animal caps. J. Cell Biol. *126*, 519–527.

39. Kishimoto, Y., Lee, K.H., Zon, L., Hammerschmidt, M., and Schulte-Merker, S. (1997). The molecular nature of zebrafish *swirl*: BMP2 function is essential during early dorsoventral patterning. Development *124*, 4457–4466.

40. Nguyen, V.H., Schmid, B., Trout, J., Connors, S.A., Ekker, M., and Mullins, M.C. (1998). Ventral and lateral regions of the zebrafish gastrula, including the neural crest progenitors, are established by a *bmp2b/swirl* pathway of genes. Dev. Biol. *199*, 93–110.

41. Nasevicius, A., and Ekker, S.C. (2000). Effective targeted gene 'knockdown' in zebrafish. Nat. Genet. *26*, 216–220.

42. Moriyoshi, K., Richards, L.J., Akazawa, C., O'Leary, D.D., and Nakanishi, S. (1996). Labeling neural cells using adenoviral gene transfer of membrane-targeted GFP. Neuron *16*, 255–260.

43. Lee, C.-H., and Gumbiner, B.M. (1995). Disruption of gastrulation movements in *Xenopus* by a dominant-negative mutant for C-cadherin. Dev. Biol. *171*, 363–373.

44. Hammerschmidt, M., Pelegri, F., Mullins, M.C., Kane, D.A., van Eeden, F.J., Granato, M., Brand, M., Furutani-Seiki, M., Haffter, P., Heisenberg, C.P., et al. (1996). *dino* and *mercedes*, two genes regulating dorsal development in the zebrafish embryo. Development *123*, 95–102.

45. Wilson, J., and Tucker, A.S. (2004). Fgf and Bmp signals repress the expression of Bapx1 in the mandibular mesenchyme and control the position of the developing jaw joint. Dev. Biol. *266*, 138–150.

46. Yamamoto, A., Amacher, S.L., Kim, S.H., Geissert, D., Kimmel, C.B., and De Robertis, E.M. (1998). Zebrafish *paraxial protocadherin* is a downstream target of *spadetail* involved in morphogenesis of gastrula mesoderm. Development *125*, 3389–3397.